



M. O. Eze and I. B. Ijeh

Department of Physics, Michael Okpara University of Agriculture, Umudike, Abia State, Nigeria

Received: October 04, 2020 Accepted: February 13, 2021

Abstract: Proton precession magnetometer of G857 model with 0.1 gamma sensitivity was used to survey a field in Michael Okpara University of Agriculture in Umudike to ascertain the magnetic fabric of the area in order to determine its Geology. Edge detection techniques such as analytical signal, tilt derivative and its associated horizontal derivative, vertical and horizontal derivatives magnetic data have delineated structural features in the area significant for hydrocarbon prospectivity in the basin. Reduction-to-Equator (RTE) of the Total horizontal derivative (THDR) of tilt derivative (TDR) revealed more magnetic anomalies that was not seen on Total magnetic intensity (TMI) map. The analytical signal has shown the location of magnetic sources, contacts or edges. Applying threshold cutoff of 0.0, to the RTE tilt grid has delineated litho-structural boundaries/contacts at the study area. The vertical derivatives map enhanced high frequency anomalies relative to low frequencies.

Keywords: Magnetometer, magnetic surveying, Edge detections, Oasis Montaj

Introduction

The data from survey is known as Potential field data (ground or aeromagnetic data) commonly maps basement structures and depth (Okiwelu et al., 2014). The relationship between the basement structures and hydrocarbon is at play in the study area (Niger Delta basin). Structural analysis of the basement can advance the understanding of the overlying structures and the petroleum system for an area (Alexander and Radovich, 2003).

The precision proton magnetometer with 0.1 gamma sensitivity does not require orientation or levelling. It utilizes the precision of spinning protons or nuclei of the hydrogen atom in a hydrocarbon fluid to measure the total magnetic intensity (Dobrin and Savit, 1998).

Geology of the area

The study area is within the Tertiary Niger Delta basin which is located in the Gulf of Guinea central West Africa. It is bounded between the latitude 5°28'29" and 5°28'24" and longitude 7°32'29" and 7°32'32" (Fig. 1). The approximate area covered by the basin is 75,000 sq km. It consists of a

regressive clastic sequence which attains maximum thickness of 12,000 m (Orife and Avbovbo, 1982). The type of Delta growth of the Niger Delta basin is the siliciclastic system of Delta which began to prograde across pre-existing continental slope into the deep seaduring the late Eocene and is still active today (Burke et al., 1971). It is bounded by the Anambra basin and Abakaliki trough to the north, the Cameroun volcanic line to the east, the Gulf of Guinea to the south and the Dahomey embayment to the west. The Tertiary sediments of the Niger Delta basin is deposited in three major sequences (Dublin-Green and Agha, 2005). The oldest sequence is the Akata formation is consists of the holomarine shale and serves as the main active source rock in the basin. The Agbada formation overlain the Akata consists of Eocene to pleistocene aged marine sand-shale sequence. The youngest sequence is the Benin formation is made up of upper coastal plain sands and a massive continental sequence. The area is situated in the Benin Formation which is one of the formation of Cenozoic Niger-Delta basin of Nigeria.

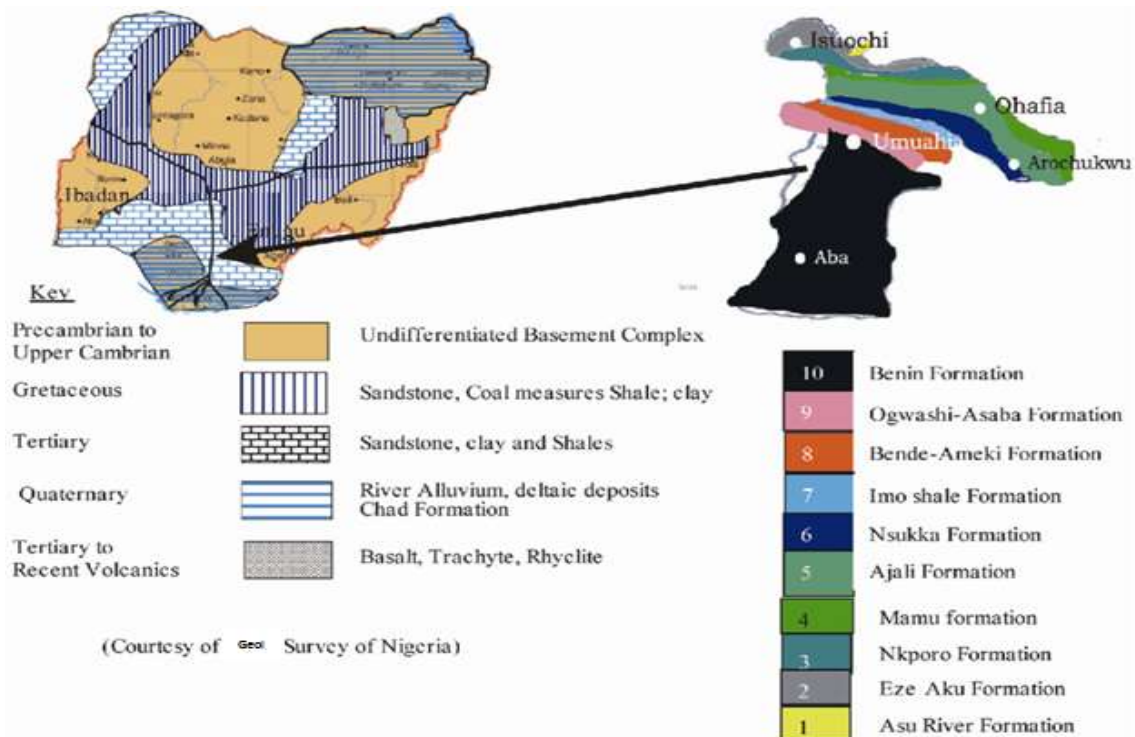


Fig. 1: Geology of the study area

Objective of the study

The purpose of this ground magnetic surveying on the Michael Okpara University of Agriculture Umudike is to identify and describe regions of the earth's crust that have these unusual (anomalous) magnetization in terms of Geology (Ozebo and Nwodo, 2017). Lateral variations of certain magnetic minerals whose distribution can bear little relation to bulk lithologic patterns cause magnetic anomalies (Lyastsky, 2010).

Materials and Method

The proton precession magnetometer unit which serves as an important function for earth science professionals was used to map the magnetic field sensitivity of Michael Okpara University of Agriculture Umudike, Abia state for academic purposes. Six profiles of ground magnetic data were obtained during a field work at Michael Okpara University of Agriculture Umudike, Abia state using a proton magnetometer of G 857 model. Magnetic readings were taken along profiles with a station interval of 10 m and with a profile spacing of 10 m. Samples were taken at 10 m interval along the 100 m. Each profile was 100 m each.

Instruments used during the field work include: Magnetic compass, Global Positioning System (GPS), Proton Magnetometer Model, Geological hammer (1 kg), sample

bags, field note book, shovels, pegs, ranging poles, measuring tape. The data were processed using oasis Montaj software 6.4 model. The necessary reduction concerning the daily variation and international (magnetic reference field, IGRF) geomagnetic corrections were performed (Selim and Aboud, 2013), the regional gradient and the time variation were applied, and then the total intensity anomaly map was constructed. Diurnal and the data were gridded using reasonable grid interval (100 m) in order to produce corrected magnetic anomaly map. The data was gridded using Minimum curvature gridding method. Minimum curvature gridding method is most suitable for potential data field data produced (Briggs, 1974). It represents data more sharply and also applies a constant known as artificial degree of smoothing to the data (Fortin *et al.*, 2017). The Total magnetic intensity map was calculated. After reduction of the magnetic anomalies to the pole, edge detection enhancement techniques were applied to the data to enhance certain characteristics of the sources. They are Analytical signal, Tilt derivatives, and its associated horizontal derivative, vertical and horizontal derivative.

Thus, reduction-to-equator was calculated and the map is less noisy and anomalies better positioned. The RTE is expressed as:

$$L(\theta) = \frac{[\sin(I) - i \cdot \cos(I) \cdot \cos(D - \theta)]^2 x(-\cos^2(D - \theta))}{[\sin^2(Ia) + \cos^2(Ia) \cdot \cos^2(D - \theta)] x [\sin^2(I) + \cos^2(I) \cdot \cos^2(D - \theta)]}, \dots \text{Equation 1}$$

(|Ia| < |I|), Ia = I

Where: I is the magnetic inclination; D is magnetic declination; L_θ is direction of wave number vector in degrees azimuth

Regional-residual separation

The airborne magnetometer has always set out to measure only the scalar magnitude of the total magnetic field (Reeves, 2005). This is the vector sum of the field attributable to the earth's core (and approximated by the IGRF) and the sum of all local effects due to the magnetization of crustal rocks. To enhance the broad features, due to deep structures, separation of residual (shallow response) from regional field, Butterworth and low-pass filter were applied to the TMI data. The common objective in this technique is to isolate regional anomaly from local features/anomalies. Regional-residual separation is good for easy delineation of shallow and deep subsurface structures (Mekkawi *et al.*, 2007).

It is a process that involves high pass spatial filtering. This filtering action gave rise to the regional and residual maps. Magnetic minerals whose distribution can bear little relation to bulk lithologic patterns are the usual carriers of rock magnetization, their lateral variations cause magnetic anomalies (Dobrin *et al.*, 1998). The residual magnetic features are related mainly to sources within the crust of the earth. The residual map reflects near-surface and high frequency components while the regional map reflects deep-seated and low frequency crustal features.

Edge detection

The study rely on enhancements that allow us interpret to see structures. They are the following derivatives, Total gradients, vertical derivatives, horizontal and Tilt Derivatives. These derivatives helped in defining the physical properties of the magnetic source structures causing anomalies at the study area (Verdezco *et al.*, 2004).

Analytical signal

Roest *et al.* (1992) showed that the amplitude (absolute value) of the 2D analytical signal at location (X, Y) can be derived from three orthogonal gradients of the total magnetic field.

The analytical signal was calculated to extract the location of magnetic sources contacts or edge. The analytical signal showed discontinuities, some of which coincide with the geological boundaries at the area. A, which is the analytical signal is given by this equation:

$$|A(x, y)|^2 = \sqrt{\left(\frac{\delta M}{\delta x}\right)^2 + \left(\frac{\delta M}{\delta y}\right)^2 + \left(\frac{\delta M}{\delta z}\right)^2} \dots \text{Eqn 2}$$

Where: M= anomalous magnetic field in horizontal and vertical directions. The analytical signal filter, an amplitude domain filter was applied to the magnetic intensity data.

Tilt derivatives

Tilt derivatives is formally used to derive the local wave number (Verduzco *et al.*, 2004), but uses the absolute value of the horizontal derivative in the denominator. The tilt derivative or tilt angle was first proposed by Miller and Singh (1994) as a tool for locating magnetic sources on magnetic profile data.

$$TDR = \tan^{-1} \frac{VDR}{THDR} \dots \text{Equation 3}$$

For profile data, $THDR = \sqrt{\frac{\partial T}{\partial X}}$ Equation 4

For gridded data, $THDR = \sqrt{\frac{\partial T^2}{\partial X} + \frac{\partial T^2}{\partial Y}}$ Equation 5

Where VDR is the first vertical derivative and THDR is the total horizontal derivative of TMI; VDR Can be negative or positive while THDR is always positive

The magnetic tilt angle is a normalized derivative based on the ratio of the vertical and horizontal derivatives of the RTP field (Salem *et al.*, 2007); in this case, RTE because the study area is a low latitude area. The tilt is restricted to value between $-\pi/2$ and $+\pi/2$ ($+90^0$ and -90^0) regardless of the amplitudes of VDR (first vertical derivative) or THDR. This fact makes this relationship function like an automatic gain control (AGC) filter and tends to equalize the amplitude output of TMI anomalies across a grid or along a profile (Verduzco *et al.*, 2004). Automatic gain control images by means of RTE of tilt derivative provide an effective alternative to vertical derivative to map continuity of structures and enhance magnetic fabric (Verduzco *et al.*, 2004). TDR of RTE crosses through zero at or near the edge of a vertical-sided source and is negative outside the source region (Miller and Singh, 1994).

Vertical derivatives

It is a high pass filter that passes all the frequencies with $k \geq Kc$. The high-pass filter attenuates the frequencies lower than the cut off frequency. In 1D Fourier domain, it is expressed as:

$$L(K) = \begin{cases} 0 & k < Kc \\ 1 & k \geq Kc \end{cases} \dots \text{Eqtn 6}$$

Where: $k \geq Kc$

Horizontal derivatives

According to Cordell *et al.*, 1985, the amplitude of the horizontal gradient is expressed as in equation 7

$$HG = \sqrt{\frac{\partial T^2}{\partial X} + \frac{\partial T^2}{\partial Y}} \dots \text{Eqtn 7}$$

Where: $\frac{\partial T}{\partial X} + \frac{\partial T}{\partial Y}$ Is horizontal derivatives of the magnetic are field in the x and y directions. The amplitude of horizontal gradient of the data is calculated in Fig. 1.

Result and Discussions

The magnetic map of the study area has exposed the geological units of the area (Boyd and Isles, 2007). The total field magnetic map has two major negative and positive local anomalies (Murari Khatiwadia, 2013), one truncated anomaly which is an indication of regional magnetic variations in the deep basement rock. On the magnetic map the predominating regional positive magnetic anomaly in northern part of the study area is related to the highly magnetic rocks of the area (Fig. 2). The TMI grid map was contoured and the closely spaced linear sub-parallel orientation of contours is an indication that there is the possibility of faults or local fractured zones passing through these areas (Chinwuko *et al.*, 2012; Eze *et al.*, 2017). Areas of strong positive anomalies on the TMI map indicate a higher concentration of magnetically susceptible minerals (principally magnetite) and is represented by the pinkish colorations (Fig. 2). Contrarily, areas with broad magnetic lows are likely areas of low magnetic concentration with lower susceptibility and is represented by bluish coloration. Generally, the high magnetic values arise from igneous and crystalline rocks. According to Gunn (1997), magnetic surveys have been mainly used in the past for mapping depth to magnetic basement of sedimentary basin and delineating igneous rock units. Recently, magnetic survey now have greater relevance to sedimentary basin studies due to some enhancements done to magnetic anomaly data (Mohammed and Mustapha, 2014). Enhancement techniques were applied to the data to enhance certain characteristics of the sources, thus facilitating the overall interpretation (Blakely, 1995). The circularly shaped magnetic anomalies

according to Gunn (1997) suggest presence of magnetic aureole within the area (Fig. 2).

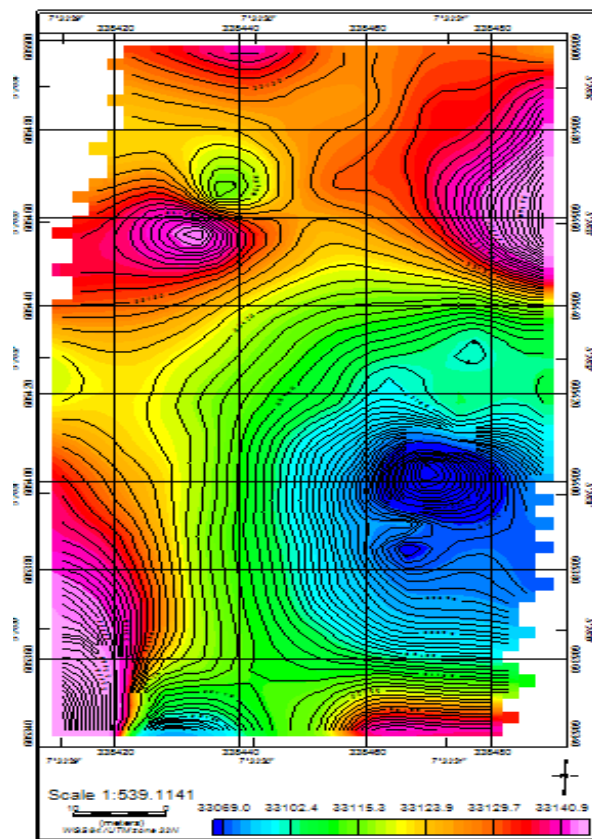


Fig. 2: The Total Magnetic Intensity (TMI) map

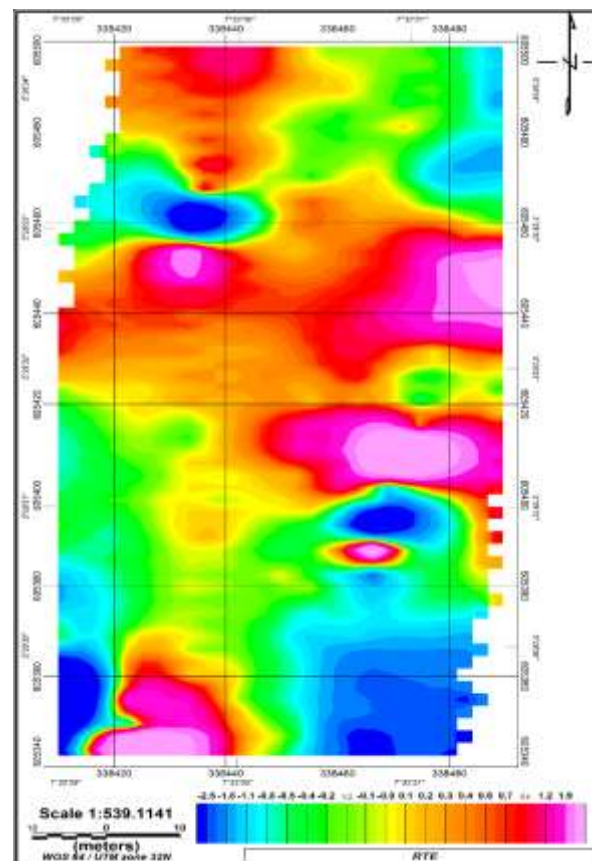


Fig. 3: Reduction to equator (RTE)

RTE: The application of reduction to equator (RTE) filter has applied a latitude dependent phase shift to centre the anomalies peak of the data (Fig. 3). Due to vector nature of the measured magnetic field, there is always polarity effect (Blakely, 1995) which manifested as a shift of the main anomaly from the center of the magnetic sources (Opara *et al.*, 2012). In other words, magnetic field itself is dipolar and usually non-vertical. The reduction to equator has preserve the image of N-S structures (Verdezco *et al.*, 2004) in the data. Because the study area, is low latitude area, the anomalies are highly truncated and the noise could be introduced (limitation of reduction-to-pole) (Macleod, 1994). The RTE is used in low magnetic latitude regions (including Nigeria) to center the peaks of magnetic anomalies over their sources making the data easier to interpret without losing any geophysical meaning. Reduction to equator map reflects the expected magnetic anomalies which translate into the amount of magnetic minerals (magnetite) presents in the rocks (Fig. 3).

Regional map: Low-pass filter was used and a cut-off wavelength of 100 m was used as threshold for separation. According to Dobrin and Savit (1998), the component of the magnetic anomaly having longer wavelength (low frequency) is referred to as regional (Fig. 4). The magnetic intensity values of the regional anomaly ranges from 33085.6 nano tesla to 33135.4 nano tesla. The regional structure is characterized by a broad negative magnetic in the southeast direction center bounded by gradients increasing towards the west and the north. These observations are an indication that the basement is deepening towards the southeast (Basseka *et al.*, 2011). The residual anomalies are due to magnetic source of shallow origin (Alagbe, 2015). These anomalies have short wavelength (high frequency).

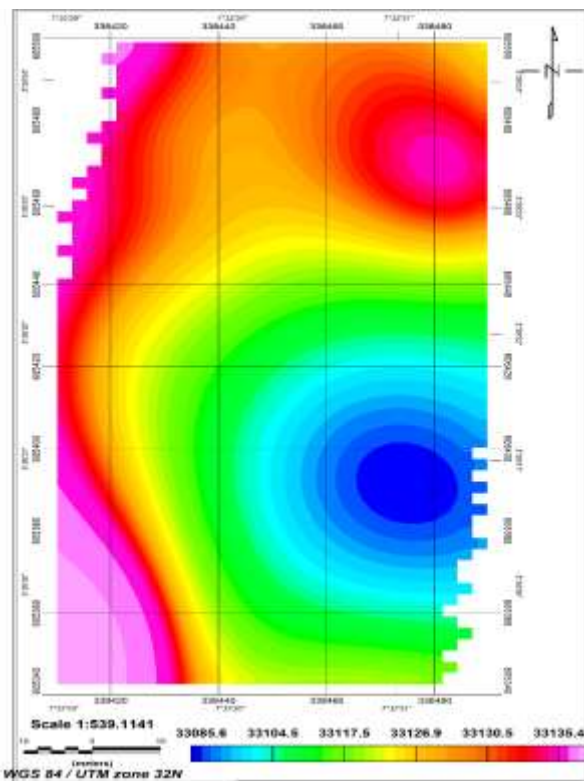


Fig. 4: Regional magnetic anomalies of MOUA field

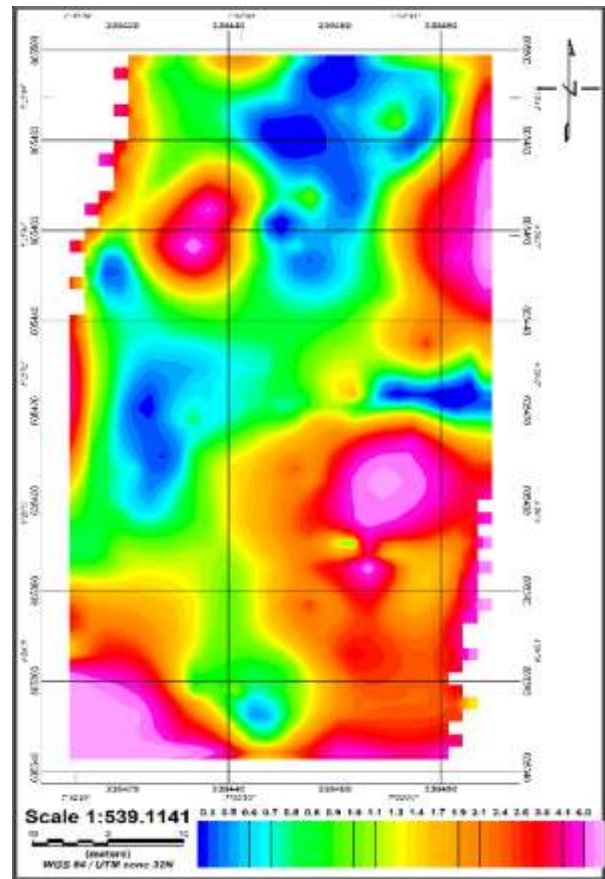


Fig. 5: Analytical signal map

Analytical signal map: The analytical signal present magnetic anomaly information stripped of the dependence on the inclination of the earth inducing field so that anomalies are positive and sit directly above their sources (Nabighian, 1972; Roest *et al.*, 1992). The analytical signal was calculated to extract the location of magnetic sources contacts or edge. This map sharpens the contact between the magnetic high and low patterns. According to Anad and Mita (2006), analytical signal was useful in locating the edges of magnetic source bodies since the study area is on the low magnetic latitude where remanance and/or low magnetic complicate interpretation (Fig. 5). Magnetic structures striking north south are difficult near the equator but the analytical signal derivative has recovered the N-S contacts at the study area. Analytical signal map show clear boundaries of major magnetized zones. It showed discontinuities, some of which coincide with the geological boundaries at the area (Fig. 5). The amplitude of the analytical signal of the total magnetic field produces maxima over magnetic contacts regardless of the direction of magnetisation (Macleod *et al.*, 1994). The amplitude of the analytical signal is related to the amplitude of magnetization. The likely area of most significant concentration of mineral deposits in this area is correlated with high analytical signal amplitude in agreement with the report of Silva *et al.* (2003).

Tilt derivative: Applying threshold cutoff of 0.0, to the RTE tilt grid has delineated litho-structural boundaries/contacts at the study area as shown in Fig. 6B.

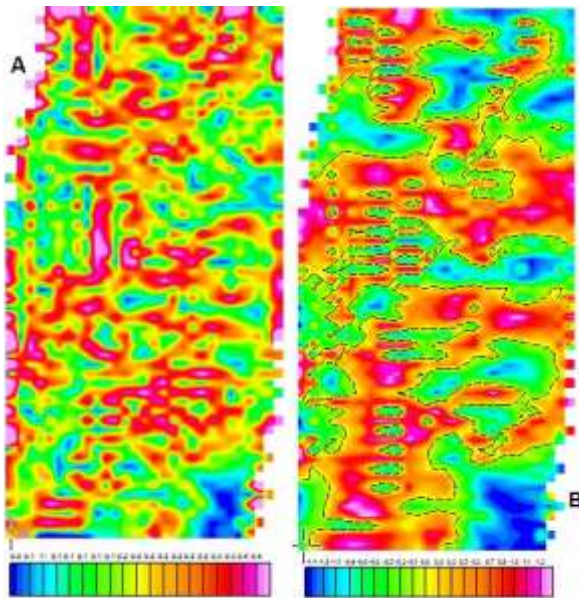


Fig. 6: A): The RTE_Tilt derivative_THDR B): RTE of Tilt derivative with zero contour lines represent litho-structural boundaries

Vertical derivative map: Derivatives essentially enhance high frequency anomalies relative to low frequencies (Adagunodo *et al.*, 2015). Vertical derivative filter was applied to the raw later and this has quantify the spatial rate of change of the magnetic directions in the vertical direction (Fig. 7).

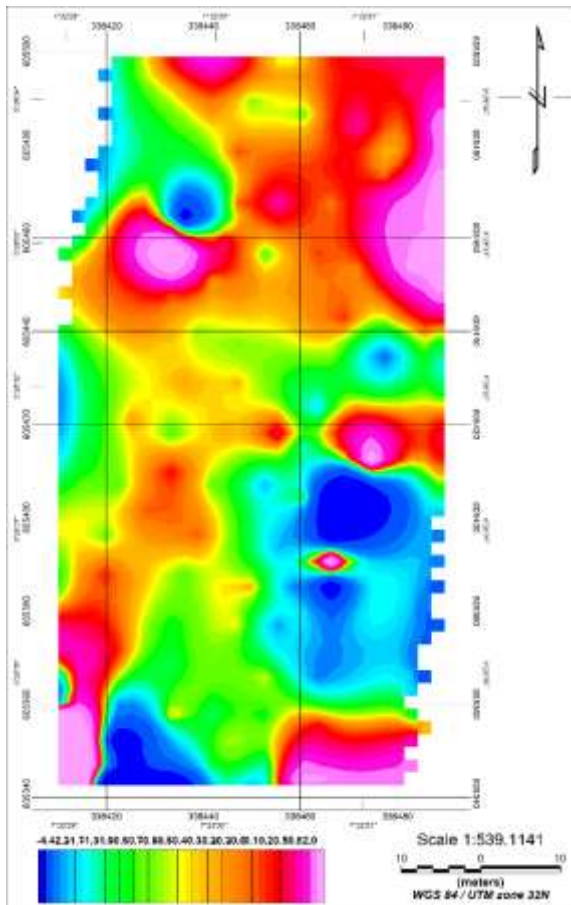


Fig. 7: Vertical Derivative map

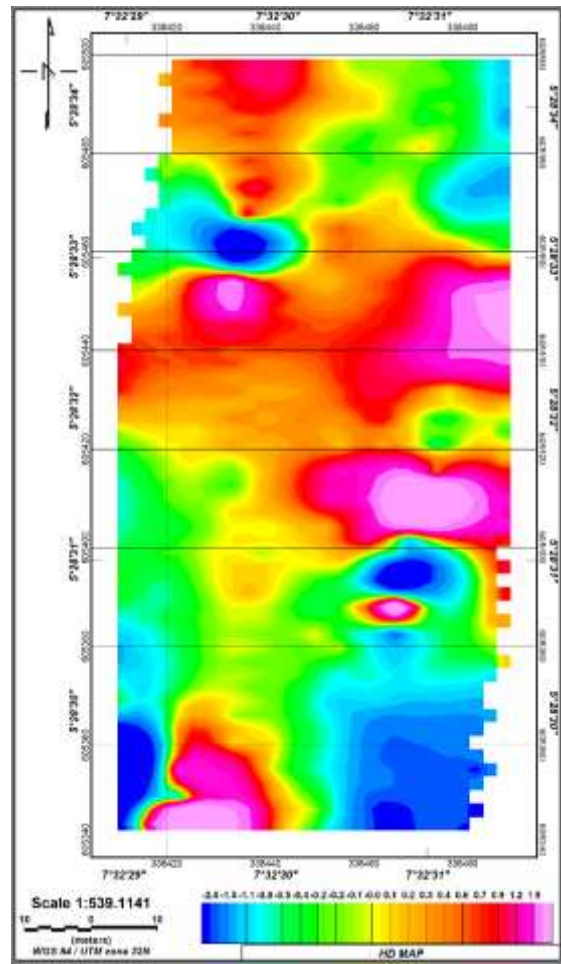


Fig. 8: Horizontal derivative map

Horizontal derivative map: The horizontal derivative filter was applied to the data to quantify the spatial rate of change of the magnetic directions in the horizontal direction. It enhances high frequency variations in the data (Fig. 8). These high frequency variations could be due to presence of faults and /or boundaries between different geological units. It is also robust method to delineate shallow and deep sources in comparison with the vertical gradient, which is useful only for the shallower structures.

Interpretation of the Profile result: The profile results of the area provides a reasonably precise estimate of the depth distribution of the magnetic sources of the area according to Erwin *et al.* (1995). The Total intensity value from the land magnetic survey of the area range from 33152 nT to 33138 (Fig. 9).

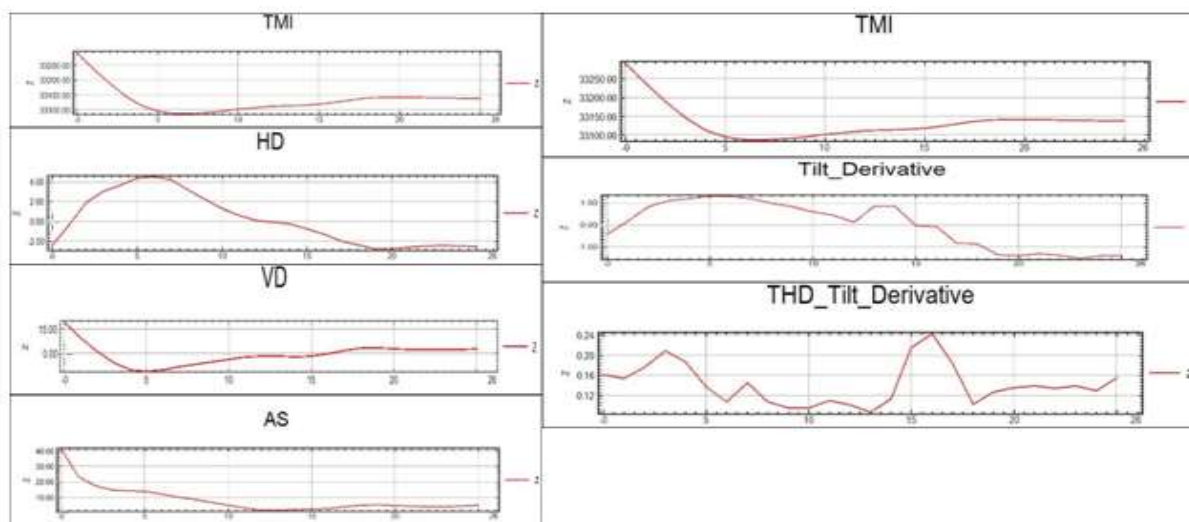


Fig. 9: Profiles comparing the response of common derivatives to both the tilt and total horizontal

Derivative of the TDR to TMI anomaly response

From Fig. 9, gotten from the grid derivative maps, the following points were observed:

The amplitude of response of the derivatives is in proportional with amplitude response of TMI anomaly. Contrarily, the amplitude response of the RTE tilt derivative and its associated Total horizontal derivative is independent of the amplitude of the TMI anomaly response; they are dependent on the inverse value of the depth to the sources. The RTE of THDR shows six symmetric shallow anomalies (Fig. 9). The profile figures of First vertical derivatives confirm it can be negative or positive while the total horizontal derivative is always positive (Fig. 9). The profile diagrams of first vertical and horizontal derivatives shows they are spatial rate of change of the magnetic directions in the vertical and horizontal directions respectively.

Shear zone: There is remarkable decrease in magnetization associated with fault and shear structures in the area as indicated by shear structures revealed by the magnetic data (Fig. 10).

Conclusion

The results from edge detection techniques revealed subtle structural features such as faults, dike-structures, fracture and shear zones lithologic contact which are significant for hydrocarbon prospectivity in the basin. Tilt derivative has been used to trace the lithologic boundary/edges in the study area. The RTE of the THDR of TDR revealed more magnetic anomalies which are symmetric shallow anomalies. Through Regional-residual separation, the deep subsurface structures have been delineated while the First vertical derivative emphasizing the effect of the near surface anomalous sources in the area. Horizontal derivative filter has also quantifies the spatial rate of change of the magnetic directions in the horizontal derivatives. The analytical signal defines clearly the maxima of major magnetic anomalies. These maxima indicate positions of magnetic contrast.

Conflict of Interest

Authors declare that there is no conflict of interest reported in this work.

References

Adagunodo TA, Sunmonu IL & Adeniji AA 2015. An overview of Magnetic method in mineral exploration. *J. Global Ecol. and Env.*, 3(1): 13-28.

Alagbe OA 2015. Depth Estimation from Aeromagnetic Data of Kam. *Int. J. Advanced Res. in Physical Sci. (IJARPS)*, 2(1): 37-52.

Alexander M, Prieto C & Radovich B 2003. Basement Structural Analysis: Key in Deep Shelf Plays. The American Oil and Gas Reporter. Retrieved from <http://www.igc.world.com>

Anand & Mita R 2006. Aeromagnetic data analysis for the Identification of concluded Uranium deposits: A case history from singhum Uranium province. *India Earth Planet space* 58: 1099-1103.

Blakely R J 1995. Potential Theory in Gravity and Magnetic Applications, Cambridge Univ. Press.

Boyd DM & Isles DJ 2007. Geological Interpretation of Airborne Magnetic Surveys-40 years on. In: proceedings of exploration 07; fifth decennial international conference on mineral Exploration” edited by B Milkereit, pp. 491-505.

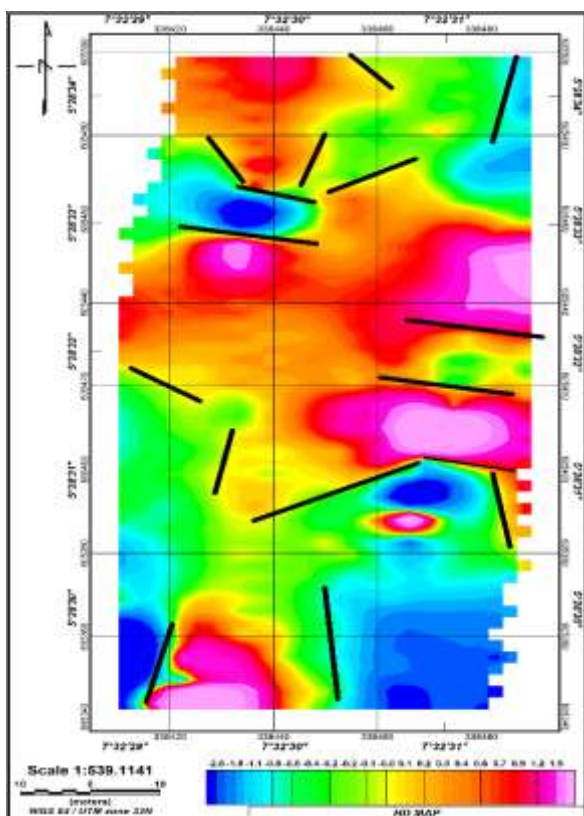


Fig. 10: Shear zone

- Briggs IC 1974. Machine contouring using minimum curvature: *Geophysics*, 45: 39-48.
- Burke K, Dessauvage TFJ & Whiteman AJ 1971. Opening of the Gulf of Guinea and geophysical history of the Benue depression and Niger delta. *Nature*, 233: 51-55.
- Charles AB, Yves S & Jean MT 2012. Subsurface structural mapping using gravity data of the northern edge of the Congo craton, South Cameroon. *GEOFIZIKA*, 28: 2011
- Chinwuko AI, Onwumesi AG, Anakuba EK, Onuba, LO & Nwaokeabia, NC 2012. Interpretation of Aeromagnetic Anomalies over parts of Upper Benue Trough and Southern Chad Basin. *Nig. Adv. Appl. Sci. Res.*, 3(3):1757-1766.
- Cordell L & Grauch VJS 1985. In: Hinze WJ (Ed.) Mapping basement magnetization zones from aeromagnetic data in the San Juan Basin, New Mexico. The utility of regional gravity and magnetic anomaly maps. *Soc. Explor. Geophys.*, pp. 181-197.
- Dobrin MB & Savit CH 1988. Introduction to Geophysical Prospecting, 4th ed. McGraw-Hill Co., p. 865.
- Dublin-Green WF & Agha GU 2005. Future Petroleum Potential of Nigeria. Document Sponsored/Printed by NNPC/Mobil.
- El Sayed IS & Essam A 2013. Application of spectral analysis technique on ground magnetic data to calculate the Curie depth point of the eastern shore of the Gulf of Suez, Egypt. *Arabian Journal of Geosciences*. 3(5).
- Erwin E, John P & Nathalie M 1995. Geophysical exploration and Development Corporation (GEDCO) *Recorder*, 20(7).
- Eze MO, Amoke AI, Dinneya OC & Aguzie, PC 2017. Basement and automatic depth to magnetic source interpretation of parts of southern Benue Trough and Anambra Basin. *IOSR J. Appl. Geol. and Geophysics*, 5(3): 67-74.
- Fortin R, Hovgaard J & Bates M 2017. Airborne Gamma-ray spectrometry in 2017: solid ground for New Development. In "Proceedings of Exploration 17: Sixth Decennial International Conference on Mineral Exploration" edited by VOL Tschirhart and MD Thomas, pp. 129-138.
- Gunn PJ 1997. Enhancement and presentation of airborne geophysical data. *AGSO J. Australian Geol. & Geophysics*, 17(2):63-76.
- Ibrahim A, Ayinla HA & Ahmed JB 2016. Geomagnetic signature and depth estimate of basement rock around Iseyin Area (Ado-Awaiye), Ibadan, Southwestern Nigeria. *J. Geogr., Evt. and Earth Sci. Int.*, 4(2): 1-12.
- Kamba AH & Ahed SK 2017. Depth to basement determination using source parameter imaging (SPI) of aeromagnetic data: An application to lower Sokoto Basin, Northwest, Nigeria. *Int. J. Modern Appl. Phys.*, 7(1): 1-10.
- Lyastsky H 2010. Magnetic and gravity methods in mineral exploration: The value of well-rounded Geophysical skills. *Recorder*, 33(08).
- Meleod IN, Jones K & Ting FD 1994. 3D analytical signal in the interpretation of total magnetic field data at low magnetic latitudes. *Exploration Geophysics*, 24: 679-688.
- Mekkawi M, Elbohoty M & Aboud E 2007. Delineation of Subsurface Structures in the area of a Hot Spring, Central Sinai, Egypt based on Magnetotelluric and Magnetic Data. *Proceeding of the 8th Conf. Geol. Sinai for Devt.*, Ismalia, pp. 29-39.
- Miller HG & Singh V 1994. Potential field tilt a new concept for location of potential field sources. *J. Appl. Geophys.*, J32: 213-217.
- Mohammed AG & Mustapha A 2014. Evaluation of the Magnetic Basement Depth over Parts of Bajoga and Environs, Northeastern Nigeria by Stanley's Method. *IOSR J. Appl. Geol. and Geophys.*, 2(4): 47-53.
- Murari K 2013. Integrated Geophysical studies of the Fort Worth basin (Texas), Harney Basin (Oregon), and Snake River Plain (Idaho) DOI 10.1007/s12517-013- Thesis submitted to the Conocophillips School of Geology and Geophysics.
- Nabighian MN 1972. The analytic signal of two dimensional magnetic bodies with polygonal cross-section: its properties and use for automated anomaly interpretation. *Geophysics* (37): 507-517.
- Okiwelu AA, Obianwu VI, Eze OE & Ude IA 2014. Magnetic anomaly patterns, fault-block tectonism and hydrocarbon related structural features in the Niger Delta basin. *IOSR J. Appl. Geol. and Geophys.*, 1: 31-46.
- Opara AI, Ekwe AC, Okereke CN, Oha IA & Nosiri OP 2012. Integrating airborne magnetic and landsat data for geologic interpretation over part of the Benin Basin, Nigeria. *The Pacific J. Sci. and Techn.*, 13(1).
- Orife & Avbovbo AA 1982. Stratigraphic and unconformity traps in the Niger Delta. *AAPG Bulletin*, (65): 251-265.
- Ozebo VC & Nwodo MU 2017. Interpretation of high resolution aeromagnetic data over Nsukka and Udi areas of Enugu state, Nigeria. *FUW Trends in Sci. & Techn. J.*, 2(1): 182 - 187.
- Reeves C 2005. Aeromagnetic surveys: Principles, practice and interpretation geosoft. Farrington JL 1952. A preliminary description of the Nigerian Lead-Zinc field. *Econ. Geol.* 47: 483-608.
- Roest WR, Verhoef & Pilkington M 1992. Magnetic interpretation using the 30 analytical signal. *Geophysics*, 57(1): 166-125.
- Salem A, Williams S, Fairhead JD, Ravat D & Smith R 2007. Tilt depth method: A simple depth estimation method using first magnetic derivatives. *The Leading Edge*, 26: 1502-1505.
- Verduzco B, Fairhead JD & Green CM 2004. New Insights into magnetic derivatives for structural mapping. *The Leading Edge*, 23: 116-119.